MEGACYCLE FREQUENCY SECOND SOUND

Thesis by

Harris A. Notarys

In Partial Fulfillment of the Requirements

For the Degree of

Doctor of Philosophy

California Institute of Technology

Pasadena, California

1964

(Submitted April 24, 1964)

ACKNOWLEDGEMENTS

I am very grateful to Dr. J. R. Pellam for suggesting this problem and providing for me the opportunity to carry out this research under his guidance.

I should also like to express my appreciation to the National Science Foundation and the Alfred P. Sloan Foundation for assistantships and financial support of this research.

ABSTRACT

Generation and detection of second sound have been extended to 25 Mc/sec using a resonant cavity technique. Investigations show the attenuation coefficient of second sound is proportional to the square of the frequency up to 1.3 Mc/sec at 1.22°K, 4 Mc/sec at 1.47°K, and 10 Mc/sec at 1.9°K - 2.1°K in agreement with Khalatnikov's theoretical predictions and with previous low frequency measurements.

TABLE OF CONTENTS

CHAPTER I

INTRODUCTION

In 1940 Tisza[1] predicted the existence of a new wave motion in liquid helium II[2-5] on the basis of his two fluid model. Independently, in 1941 Landau[6] also predicted it from his quantum hydrodynamic theory. It was not until Lifshitz[7] stressed the thermal wave aspects of this wave motion and showed that the most efficient generation technique for it was a heater, that Peshkov[8] first observed second sound and measured its velocity.

Subsequently, second sound has been investigated in great detail. The velocity[9-17] has been measured by various means and the attenuation[18-20] has been measured by a number of investigators. The theory of second sound attenuation has been derived by Landau and Khalatnikov[21-23] from Landau's theory of liquid helium II and has been found to agree remarkably well with experiment.

However, in all the previous experimental investigations of second sound the highest frequencies used were those of Hanson and Pellam[19] who worked between 100 kc/sec and 280 kc/sec*. Hence, the properties of second sound at frequencies above this are open to experimental investigation. Furthermore, the high frequency range of

---

* Frequencies up to 600 kc/sec were reported by Mercereau, Notarys and Pellam[17] using a diffraction technique. However, those frequencies were attained in the initial stages of this investigation.

second sound could provide a useful tool for the microscopic examination of liquid helium II (at 25 Mc/sec and 1.95°K, λ_{ss} = 7200 Å).

It was on the basis of these considerations that this investigation was begun.

CHAPTER II

EXPERIMENTAL APPARATUS

Because of the high attenuation and short wavelength of second sound at high frequencies, a modified cavity technique was used for this investigation. The cavity consisted of two closely spaced quartz optical flats as the reflecting surfaces, one with a second sound emitter and the other with a second sound detector, and no side walls because of the small angular spreading of the second sound beam. A typical emitter and detector for second sound are shown in Fig. 1.

The emitter consists of a thin gold film (approximately 100 Å thick and 0.32 cm square) evaporated on a rectangular (2.5cm x 1.2cm by 0.6cm thick) quartz flat (flat to 1/8 λ). The leads to the gold emitting area are 1000 Å thick evaporated Sn films which go superconducting and hence, support no voltage drop. The second sound is generated by Joule heat from the gold surface when it is driven with an ac current.

The detector* consists of a thin film superconductor less than 800 Å thick and typically 2.5×10^{-2}cm wide and 0.24cm long evaporated on a quartz flat. The leads are again 1000 Å Sn films. With a constant current running through the detector, a temperature fluctuation of the superconductor, while it is in its transition temperature region, generates a resistance fluctuation and, hence, a voltage which is amplified and recorded.

---

* See Appendix A.

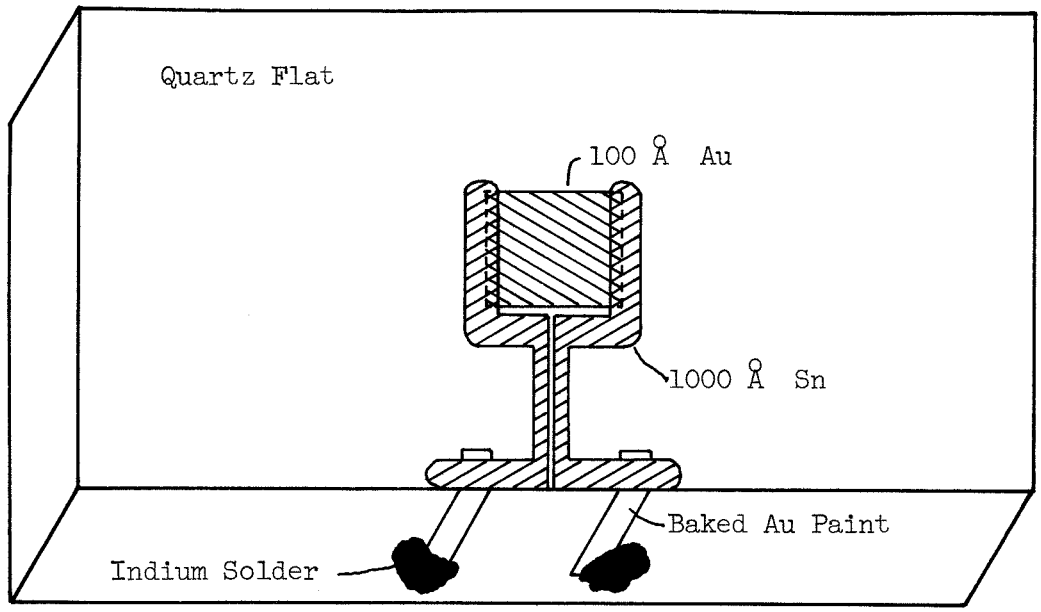

EMITTER

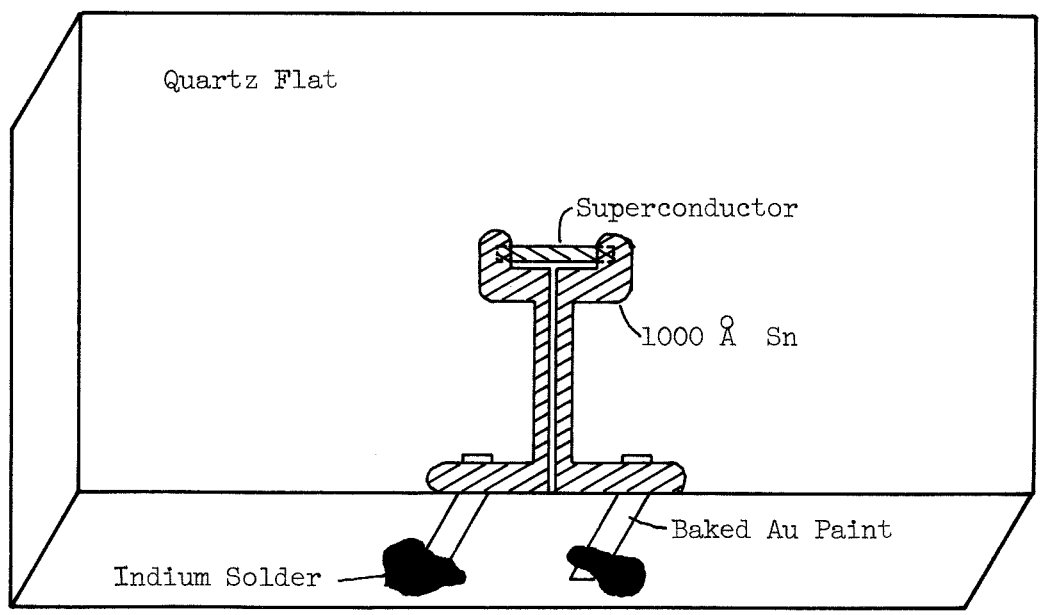

DETECTOR

FIGURE 1

The quartz flats are spaced by various methods. For spacings greater than 1/2 mm, small quartz spacers are used; between 2.5×10^{-3}cm and 12.5×10^{-3}cm formvar-coated copper wire is used; and below 2.5×10^{-3}cm tungsten wire is used. The spaced quartz flats are held in a spring-loaded clamping assembly. Fine coaxial cables from the rest of the electronics are then indium-soldered to baked gold paint films which make electrical contact to the emitter and detector films.

A block diagram of the electronic system is shown in Fig. 2. A signal generator (HP606A, HP200CD, or GR1330A) drives a current at rf frequency $\omega/2$ through the emitter and a matching resistance, R. A filter is used to suppress any harmonic, ω, in the rf current from the signal generator and the frequency is measured by a counter or a meter. Second sound at frequency ω is generated by the emitter and causes a resistance fluctuation in the detector at the same frequency. A constant dc current and a constant ac current at frequency ω_M (200 cps - 1 kc/sec from an HP200CD), passed through the detector, change the resistance fluctuation into a modulated rf voltage. (The percent modulation is determined by the ratio of ac current to dc current and the resistance properties of the detector.) The voltage from the detector is amplified and demodulated by a radio receiver (National HR060). The amplitude of the demodulated signal is then measured on a four cycle wide wave analyzer (GR736A) at ω_M or $2\omega_M$, depending on the percent modulation, and recorded.

The temperature is determined by measuring the pressure above the liquid helium bath with an oil manometer (dibutyl phthalate) and

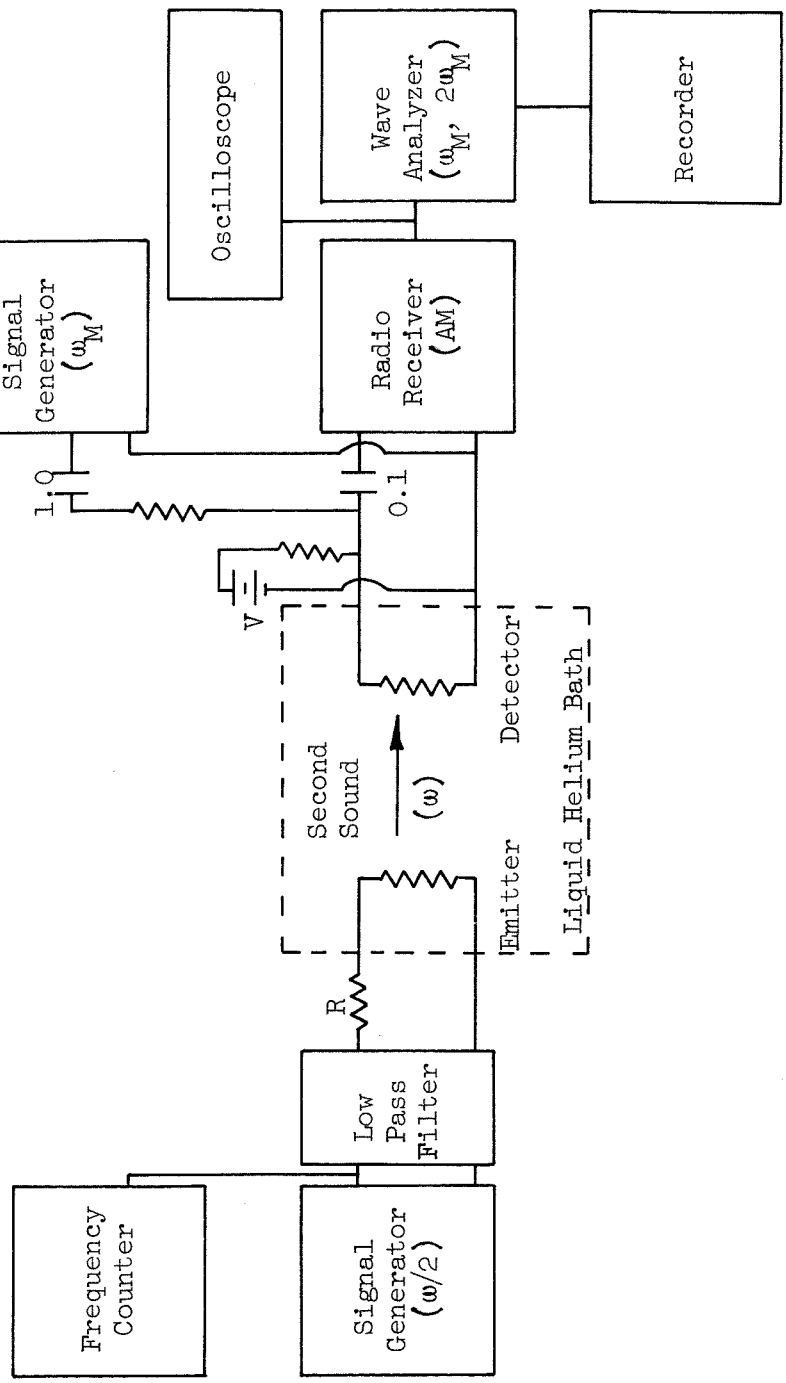

Block Diagram of Electronics

FIGURE 2

using the "1958 He^4 Scale of Temperatures" vapor pressure tables to convert.

CHAPTER III

METHOD OF MEASUREMENT

The information that can be obtained using the cavity equipment already described will now be considered.

As a close approximation to the experimental apparatus an infinite plane emitter and an infinite plane perfect reflector, with a small sensing area on it, are assumed. The amplitude of a second sound plane wave traveling the x direction can be expressed in the form $e^{-\alpha x} e^{j\omega(t-x/u_2)}$, where α is the amplitude attenuation coefficient and u_2 is the velocity. [Previous measurements of α/ω^2, which is a function of temperature only, (and not frequency) and u_2 are given in Fig. 3 for the temperature range to be considered.] For an input power per unit area of $(\dot{Q}/A)\cos\omega t$ at the emitter, the second sound temperature amplitude generated at the detector of the resonant cavity is

$$\Delta T_{ss} = \left(\frac{\dot{Q}}{A}\right) \frac{1}{\rho c u_2} \frac{1}{\left[\cosh^2 \alpha D - \cos^2 \frac{\omega D}{u_2}\right]^{\frac{1}{2}}} \cos\left[\omega t - \tan^{-1}\left(\coth \alpha D \tan \frac{\omega D}{u_2}\right)\right] \tag{1}$$

where

$(\dot{Q}/A)$	power/unit area at the emitter
ρ	density of liquid helium
c	specific heat of liquid helium
u_2	velocity of second sound

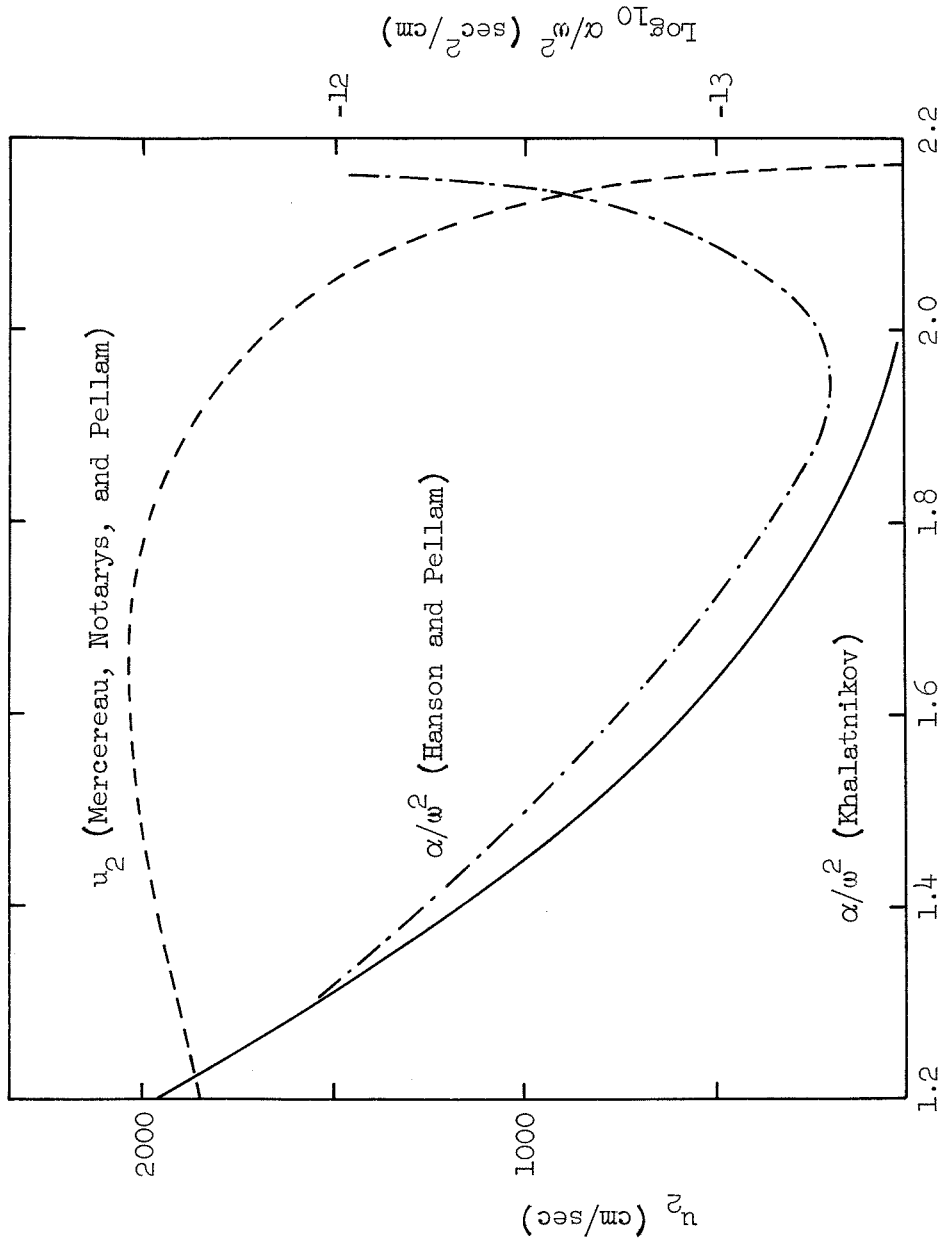

u_2 and α/ω^2 versus Temperature

FIGURE 3

α amplitude attenuation coefficient of second sound

D spacing of cavity plates

ω second sound frequency

Then, the voltage generated at the detector for a constant ac current, $I_o \cos\omega_M t$, passed through the detector is

$$\Delta V = I_o \frac{dR}{dT} \Delta T_{ss} \cos\omega_M t \qquad (2)$$

where dR/dT is the slope of the resistance versus temperature curve of the detector and ΔT_{ss} is given by Eq. (1). Hence, the voltage output is proportional to the amplitude of the second sound in the cavity. Notice that the detector is amplitude and phase sensitive and not intensity sensitive!

Equation (1), which is a typical equation for a resonant system and approximates the experimental conditions, is now examined.

For fixed cavity spacing, D, the resonance condition $\omega D/u_2 = n\pi$ (where the integer $n \geq 1$ gives the number of half wavelengths in the cavity) can be reached by varying either the frequency or the temperature (i.e. velocity). By using the resonance condition for a cavity of known spacing, D, an accurate determination of the velocity and dispersion can be made by

1) measuring the fundamental and its harmonics at a fixed temperature,

2) measuring the resonance temperatures of a fundamental and its harmonics.

On the other hand, the value of the attenuation coefficient can be determined by measuring the width of the resonance curves ($\Delta\omega_{width}$ or ΔT_{width}) at $1/\sqrt{2}$ of the peak amplitude and using the relevant expansion of Eq. (1)

1) for the frequency-resonance curve (temperature constant)

$$\alpha/\omega^2 = \frac{\Delta\omega_{width}}{\omega^2}\,\frac{1}{2u_2} \tag{3}$$

2) for the temperature-resonance curve (frequency constant)

$$\alpha/\omega^2 = \frac{\Delta T_{width}}{2}\,\frac{1}{\omega}\,\frac{du_2/dT}{u_2^2} \tag{4}$$

where du_2/dT is the slope of the velocity versus temperature curve of second sound. Hence, for those frequencies that have well-defined resonances, the position of the resonance and its width give accurate measurements of the velocity and attenuation coefficient of second sound.

At higher frequencies, when the resonances are not well-defined, it is necessary to fit the experimental results to Eq. (1) in order to determine the velocity and the attenuation coefficient.

For even higher frequencies Eq. (1) loses its resonance features and becomes merely a decaying wave of form

$$\Delta T_{ss} \approx 2\left(\frac{\dot{Q}}{A}\right)\frac{1}{\rho c u_2}\,e^{-\alpha D}\cos\left(\omega t - \frac{\omega D}{u_2}\right) \quad . \tag{5}$$

It should be noted that in all this, D, the spacing of the cavity, is actually a possible variable, which can be used to vary the limits of the three frequency ranges considered above and, especially, to extend to higher frequencies the well-defined resonance range. Furthermore, use of the variable D (and also ω) permits the determination, or at least an estimate of, the reflection coefficient of second sound impinging on a quartz flat [which has been neglected in Eq. (1)].

If two emitters with detectors opposite them are placed in the same cavity, it is possible to determine the misalignment of the cavity by comparing the resonance frequency of the two emitter-detector sets. Also, from the second sound crosstalk between the emitter-detector sets and the variation of D and ω, the effect of diffraction and spreading of the second sound beam may be assessed.

Consequently, the approximate Eq. (1) permits the determination of the velocity and the amplitude attenuation coefficient of second sound, while the neglected effects of reflection, cavity misalignment, and spreading and diffraction of second sound can be handled experimentally.

CHAPTER IV

RESULTS AND DISCUSSION

A. Second Sound Frequency Range

With the described cavity technique, generation and detection of second sound have been extended to the frequencies given below:

$T(^{\circ}K)$	Second Sound Frequency Observed (Mc/sec)	Cavity Spacing, D (cm)
1.9 - 2.1	25	1.62×10^{-3}
1.76	17	2.93×10^{-3}
1.47	6.5	2.93×10^{-3}
1.22	3	2.93×10^{-3}

Although second sound has now been observed up to these frequencies, the actual measurement range is smaller because of two experimental difficulties.

First, at low frequencies, the frequency and temperature-resonance curves give multiple resonance peaks instead of single resonance peaks. This effect is observed below 1.2 Mc/sec for $D=7.8 \times 10^{-3}$cm at $1.9^{\circ}K$ - $2.1^{\circ}K$, but is not observed down to 160kc/sec for $D=2.93 \times 10^{-3}$cm below $1.47^{\circ}K$. While this splitting of the peaks is suppressed by increasing the second sound frequency or increasing the cavity spacing, D, emitter-detector geometry changes generally give a variation but little suppression of the splitting. The most significant feature associated with this peak

splitting is that it gives rise to second sound crosstalk between two emitter-detector sets in the same cavity whereas there is no crosstalk if there is no splitting. The effect appears to be a diffraction effect (possibly similar to laser modes[33]). Since in Eq. (1), which gives the form of the resonances in the cavity, any diffraction or possible cross modes have been completely ignored, a more careful analysis may show the origin of the difficulty. However, if the measurements are made with sufficient cavity separation and high enough frequency, the entire problem can be considered an interesting observation to be investigated at some future date.

Second, at high frequencies, the electromagnetic fields of the emitter effect the detector either by eddy current heating or magnetic field effects on the superconductor. These effects act on the detector exactly like second sound, and as the frequency increases, become more important, since the second sound signal decreases and the electromagnetic noise increases. Figures 4 and 5 show that at a given frequency, as the temperature in the above $1.9^{\circ}K$ range is increased, (the attenuation of second sound is increased) the second sound/electromagnetic noise ratio decreases and the effect becomes more marked. As the temperature is permitted to drift the noise alternately adds and subtracts from neighboring resonance peaks, since they are 180° out of phase. Finally, at high enough temperatures for the electromagnetic noise to be larger than the second sound, an oscillating signal results with maxima spaced two second sound resonances apart. Figures 4 and 5 also show the effect as frequency is increased

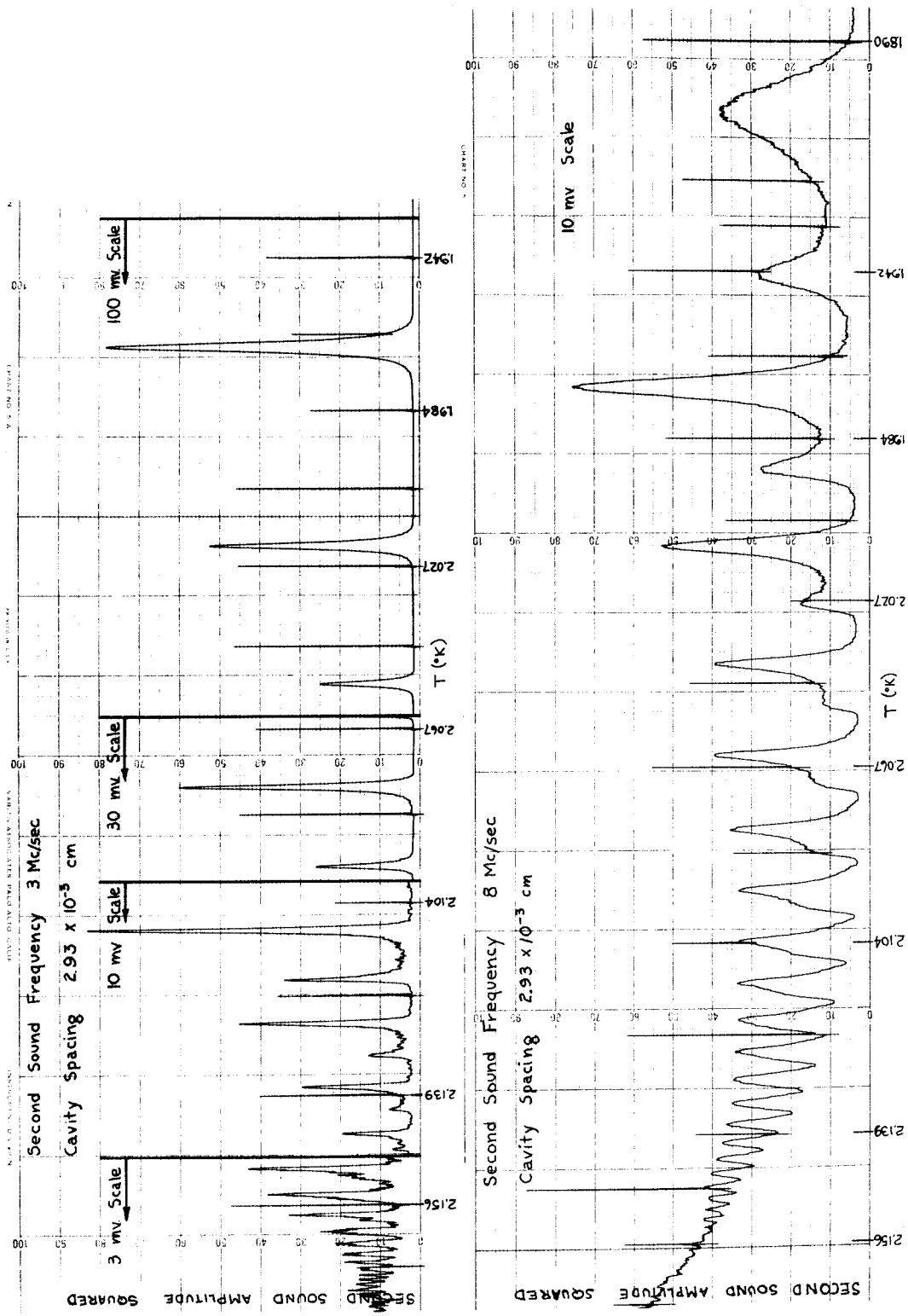
Second Sound Frequency 3 Mc/sec
Cavity Spacing 2.93 x 10⁻³ cm
3 mv Scale
10 mv Scale
30 mv Scale
100 mv Scale
SECOND SOUND AMPLITUDE SQUARED
T (°K)
2.156
2.139
2.104
2.067
2.027
1.984
1.942
Second Sound Frequency 8 Mc/sec
Cavity Spacing 2.93 x 10⁻³ cm
10 mv Scale
SECOND SOUND AMPLITUDE SQUARED
T (°K)
2.156
2.139
2.104
2.067
2.027
1.984
1.942
1.890

FIGURE 4

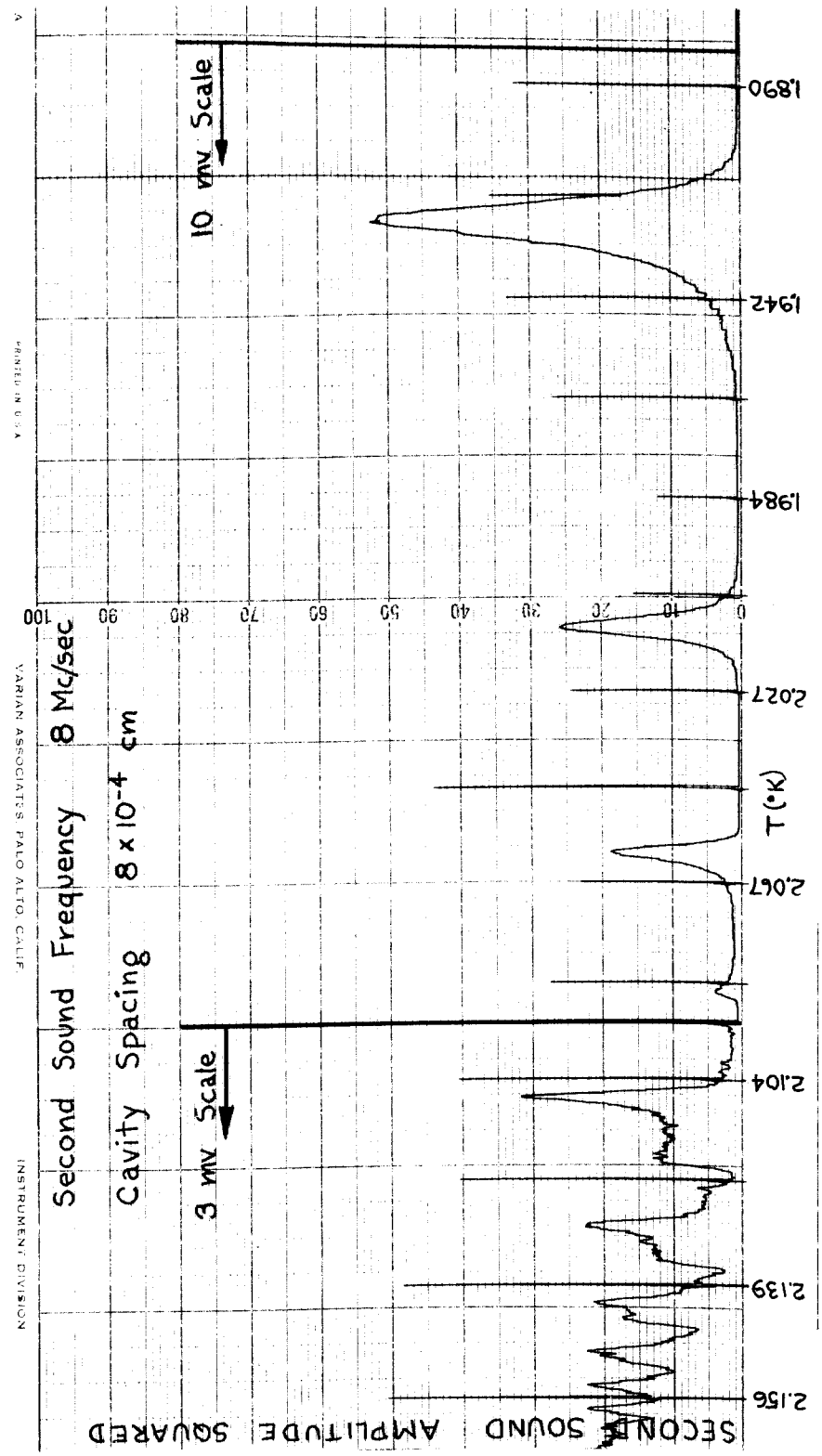
SECOND SOUND AMPLITUDE SQUARED
2.156
2.139
2.104
2.067
2.027
1.984
1.942
1.890
T (°K)
0
10
20
30
40
50
60
70
80
90
100
10 mv Scale
3 mv Scale
Second Sound Frequency 8 Mc/sec
Cavity Spacing 8 x 10⁻⁴ cm
VARIAN ASSOCIATES PALO ALTO CALIF.
INSTRUMENT DIVISION
PRINTED IN U.S.A.

FIGURE 5

and as the cavity spacing is changed. A number of designs of second sound emitters and detectors to minimize inductive and capacitive coupling by geometry were tried, but with no great success. A solution of this problem is to design an emitter which is shielded electromagnetically from the detector. However, for this investigation sufficient information is available without this added subtlety, since analysis shows that the width of a resonance curve is uneffected (within 1.5%) by pick-up signals less than 60% of the size of the second sound signal. (This analysis consists of determining the ranges of phase and amplitude of a noise signal, added to the second sound signal, which give a resultant with the qualitative features of Fig. 4 and 5.)

B. Variation of the Velocity of Second Sound with Frequency

The velocity of second sound versus temperature was measured with the cavity system in the frequency range 100 kc/sec to 340 kc/sec and the measurements agreed very well (within 1%, which is good agreement for absolute values) with those of Mercereau, Notarys, and Pellam[17], measured by a diffraction technique. The velocity change with frequency was determined by comparing the resonance temperatures of harmonics of the cavity. The results showed:

1.9861°K	$\lvert\Delta u_2/u_2\rvert \leq 0.1\%$	1.87 Mc/sec - 7.5 Mc/sec	$D = 1.6 \times 10^{-3}$ cm
2.0385°K	$\lvert\Delta u_2/u_2\rvert \leq 0.15\%$	300 kc/sec - 7 Mc/sec	$D = 7.83 \times 10^{-3}$ cm

Hence, up to 7.5 Mc/sec the velocity is constant to less than 0.15% at 2°K.

C. Variation of α/ω^2 with Frequency

α/ω^2, which has been found to be independent of frequency up to 100 kc/sec - 280 kc/sec in previous measurements, was measured as a function of frequency at several temperatures. For the determination of α/ω^2, the frequency-resonance curves were used below $1.47^{\circ}K$, while from $1.9^{\circ}K$ to $2.1^{\circ}K$ the temperature-resonance curves were used.

In Fig. 6 the measured values of α/ω^2 from 300 kc/sec to 1.3 Mc/sec at $1.22^{\circ}K$ are compared to Khalatnikov's[23] theoretical values which agree well with experiments up to 20 kc/sec.[18,20] The values show no change in α/ω^2 over the frequency range measured and agree within experimental accuracy with Khalatnikov's theoretical values. It should be noted that the wavelength of second sound, λ_{ss}, at $1.22^{\circ}K$ and 1.3 Mc/sec is 14.2×10^{-4}cm while the phonon mean free path, ℓ_{ph}, is 1.7×10^{-4}cm. Hence $8\ell_{ph} \simeq \lambda_{ss}$. By decreasing the cavity spacing it may be experimentally possible to examine phonon mean free path effects at $1.22^{\circ}K$.

In Fig. 7 the measured values of α/ω^2 from 340 kc/sec to 4 Mc/sec at $1.47^{\circ}K$ are compared to the values measured by Hanson and Pellam[19] from 100 kc/sec to 280 kc/sec. The values show no change in α/ω^2 over the frequency range measured and agree within experimental accuracy with the values of Hanson and Pellam.

In Fig. 8 the measured values of α/ω^2 from 3 Mc/sec to 10 Mc/sec in the temperature range $1.9^{\circ}K$ - $2.1^{\circ}K$ are compared to the values measured by Hanson and Pellam[19] from 100 kc/sec to

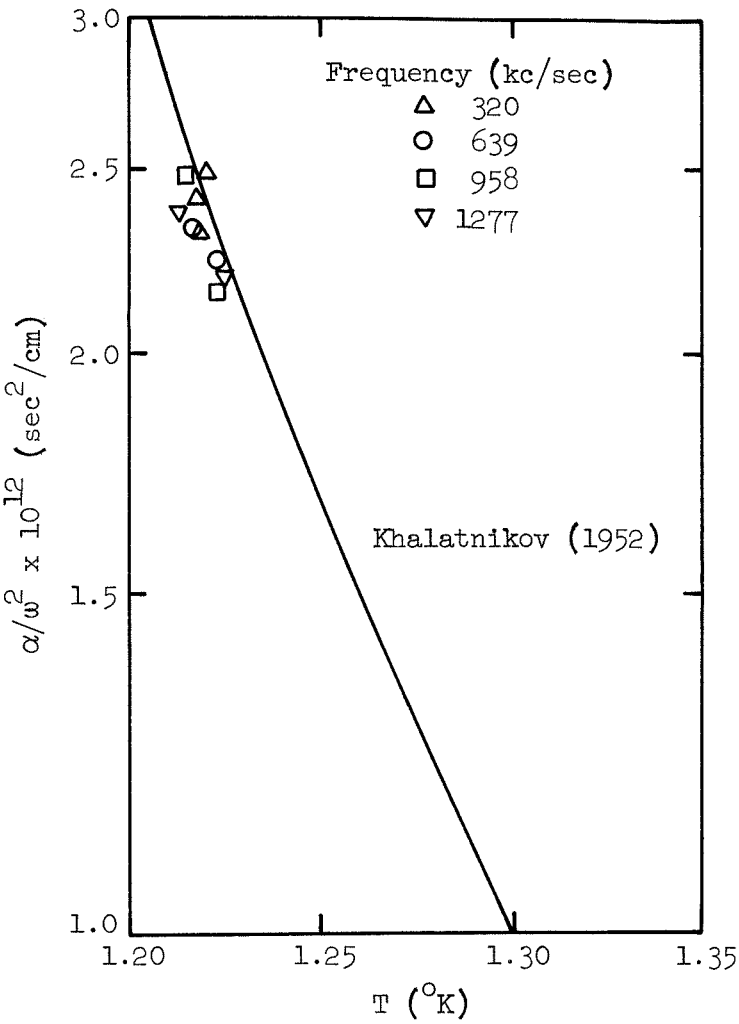

α/ω^2 versus T for Various Frequencies

FIGURE 6

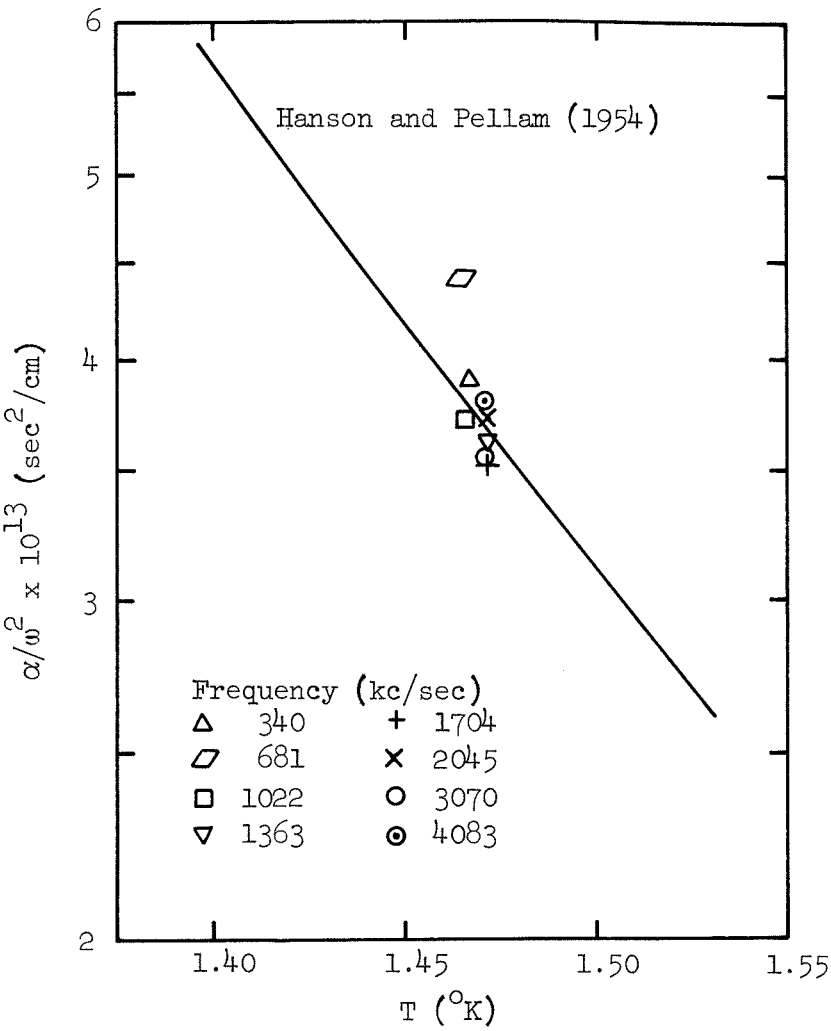

α/ω^2 versus T for Various Frequencies

FIGURE 7

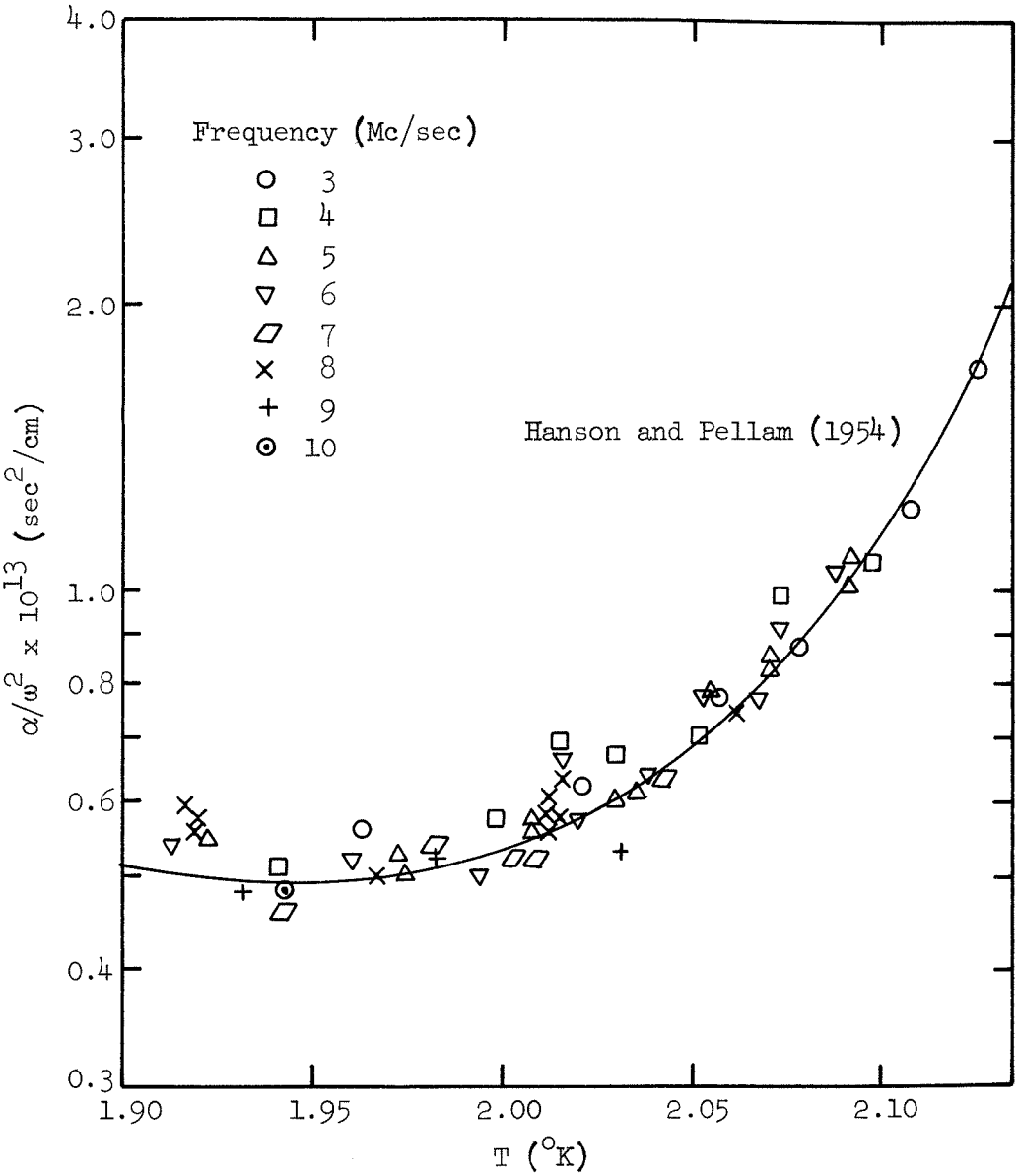

α/ω^2 versus T for Various Frequencies

FIGURE 8

280 kc/sec. The values show no change in α/ω^2 over the frequency range measured and agree with Hanson and Pellam to within experimental accuracy.

Hence, the measurements indicate that α/ω^2 is independent of frequency up to 1.3 Mc/sec at $1.22^{\circ}K$, up to 4 Mc/sec at $1.47^{\circ}K$, and up to 10 Mc/sec in the temperature range $1.9^{\circ}K$ - $2.1^{\circ}K$. This is in agreement with Khalatnikov's theoretical prediction that above $1.2^{\circ}K$ for frequencies below 100 Mc/sec the attenuation coefficient is proportional to frequency squared.

On the basis of Landau's excitation spectrum in liquid helium II, Landau and Khalatnikov found that three terms contributed to the attenuation of second sound:

1) a first viscosity term which is associated with elastic interactions,

2) a second viscosity term which is associated with the number equilibrium of the excitations through inelastic interactions,

3) an effective heat conductivity term which is as large as the combined first and second viscosity terms.

In the analysis it was shown that the longest relaxation times above $1.2^{\circ}K$ are $< 10^{-8}$ sec and are associated with the establishment of number equilibrium. Consequently, no dispersion should be observable below 100 Mc/sec. However, this analysis does not take into consideration mean free path effects which, Khalatnikov asserts, should occur at lower frequencies.

D. Nonlinear Effects

As the amplitude of the temperature oscillations in a cavity increases, the second sound amplitude attenuation coefficient increases. Consequently, in order to obtain the zero power values of α/ω^2 (given above), it is necessary to correct for the amplitude of the temperature oscillations. The fractional change of α/ω^2 with input power to the cavity has been found to be linear.[20] If the amplitude of $\rho c u_2(\Delta T_{ss})$ from Eq. (1) is denoted by ΔP_{ss} (amplitude of power/cm^2 necessary to generate the same second sound amplitude in the non-cavity case, i.e., pure traveling wave case), then, the fractional change of α/ω^2 per unit ΔP_{ss} (in watts/cm^2) for the temperature ranges considered is found experimentally to be

$\Delta(\alpha/\omega^2)/(\alpha/\omega^2) = 1.2\Delta P_{ss}$ $\quad 1.38^{\circ}K - 1.46^{\circ}K \quad \Delta P_{ss} \leq 1.2$ watts/cm^2

$\Delta(\alpha/\omega^2)/(\alpha/\omega^2) = 2.4\Delta P_{ss}$ $\quad 1.9^{\circ}K - 2.1^{\circ}K$

No associated change of velocity ($|\Delta u_2/u_2| \leq 0.002$) was observed with this change of attenuation, e.g., at $1.46^{\circ}K$ for $\Delta P_{ss} \leq 1.2$ watts/cm^2.

Since there is an added attenuation as the second sound amplitude is increased, harmonics of the generated second sound frequency should exist and have been observed. It is possible, with the present technique, to Fourier analyze large amplitude second sound. Consequently, by considering the nonlinear terms of the hydrodynamic equations this technique should be a sensitive means of determining their validity. It should be noted that the velocity change due to second sound amplitude effects has been treated theoretically by Khalatnikov[25,26] and Temperley[24] and has been measured for pulses by Dessler and Fairbank.[10]

E. Reflection Coefficient

In Eq. (1) the effects of the reflection coefficient of second sound impinging on quartz have been completely neglected. If a reflection coefficient $r = e^{-\beta}$ ($r=1$, $\beta=0$; $r=0$, $\beta=\infty$) is assumed, Eq. (1) takes the form

$$\Delta T_{ss} = \left(\frac{\dot{Q}}{A}\right)\left(\frac{1}{\rho c u_2}\right)\left(\frac{e^{\beta}+1}{2}\right)\frac{1}{\left[\cosh^2(\alpha D+\beta)-\cos^2\frac{\omega D}{u_2}\right]^{\frac{1}{2}}}\cos\left[\omega t-\tan^{-1}\left(\coth(\alpha D+\beta)\tan\frac{\omega D}{u_2}\right)\right] \tag{6}$$

where experimentally $r \simeq 1$, $\beta \simeq 0$. The attenuation coefficient from the resonance curve widths is now given by

$$\frac{\alpha}{\omega^2}+\frac{\beta}{\omega^2 D}=\frac{\Delta\omega_{width}}{\omega^2}\frac{1}{2u_2} \qquad \frac{\alpha}{\omega^2}+\frac{\beta}{\omega^2 D}=\frac{\Delta T_{width}}{2}\frac{1}{\omega}\frac{du_2/dT}{u_2^2} \tag{7}$$

Hence, as ω or D are increased, the effect of β on α/ω^2 is decreased.

Within experimental accuracy it was found, by both D and ω changes, that below $1.47^{\circ}K$ there are no measurable losses due to reflection above 160 kc/sec (lower frequencies were not considered). In the $1.9^{\circ}K$-$2.1^{\circ}K$ temperature range the same was true above 2 Mc/sec. For example, by using Eq. (7) and the scatter of α/ω^2 (0.3×10^{-13}) in Fig. 7, β is found to be less than 5×10^{-4} at $1.47^{\circ}K$. Furthermore, the data for α/ω^2 at $1.47^{\circ}K$ with a cavity spacing, D, changed to 6.05×10^{-3}cm from 2.73×10^{-3}cm fall within the values given in Fig. 7 giving no observable effect of β

with D change.

Although the effects of reflection can be ignored under the circumstances of this specific investigation, analysis of reflection in terms of the thermal properties of the materials used and the Kapitza boundary resistance[27] permits the determination (or at least an indication of the magnitude) of the thermal properties of quartz and its thermal coupling to liquid helium II.

F. Cavity Alignment

Cavity misalignment can be measured by using two emitter-detector sets in the same cavity. In a typical cavity with separation 6.05×10^{-3}cm, using formvar-coated copper wire as spacers, there was a misalignment of 4800 Å/cm (where 1000 Å/cm misalignment can be detected). The effect of misalignment should decrease with increasing frequency, i.e., increasing attenuation. For frequencies above 160 kc/sec below 1.47°K and above 2 Mc/sec in the 1.9°K-2.1°K temperature range, no effect due to misalignment has been observed.

G. Critical dc Power Effects

The second sound generation method used in this investigation has associated with it a steady heat input. Consequently, second sound measurements are valid only when the dc power input can flow out of the cavity without affecting it. Measurements of the permissible dc power input have been made by examining the temperature in the cavity using the second sound resonance temperatures and also the detector resistance. As an example, the values of these maximum

permissible power inputs for a cavity with a spacing of 2.93×10^{-3}cm and an emitter 0.32cm square are:

T(^{o}K)	Power Input (mw/cm^2)
1.22	12
1.3	22
1.4	42
1.9	125
2.0	125
2.1	84
2.15	35
2.1720	0

The powers used during the measurement of u_2 and α/ω^2 of second sound were well below the values which cause temperature changes in the cavity. However, it should be noted that the ultimate limit of this cavity technique (if not the second sound itself) is the size to which the spacing can be decreased while still permitting sufficient power to generate measurable second sound.

CHAPTER V

CONCLUSIONS

A beginning has been made in the examination of megacycle frequency second sound. Measurements have been made of the attenuation coefficient up to 10 Mc/sec (λ_{ss} = 18000 Å at 1.95°K) and the velocity up to 7.5 Mc/sec. Although there was too much electromagnetic noise for measurements to be made, second sound has been generated and detected up to 25 Mc/sec (down to λ_{ss} = 6000 Å at 2.05°K). With a more refined generation technique, higher frequencies appear to be attainable. This presents an excellent opportunity to examine liquid helium II on a microscopic scale with a probe smaller than the wavelength of visible light.

APPENDIX A

MEGACYCLE FREQUENCY SECOND SOUND DETECTORS

Because of the small wavelength, high attenuation, and dc heat flow associated with megacycle frequency second sound, most detection schemes used in previous investigations are not applicable. Hence, after careful consideration, a bolometer was chosen to satisfy the stringent requirements of this investigation.

Use of a bolometer is a common technique for detecting second sound. In the past the bolometer materials used have fallen into two classes; first, semiconductor materials such as carbon films and germanium, and second, superconductors in the form of phosphor bronze wire.[28] All the previous investigations have been at low enough frequencies so that there was no problem with thermal response of the materials used. However, approximately 500 kc/sec second sound is the upper frequency limit of these materials without special handling or considerations. Nevertheless, it is possible to extend the use of bolometers as second sound detectors into the megacycle frequency range by using evaporated thin films.

The two classes of bolometer materials mentioned above act quite differently at low temperatures. The resistance of a semiconductor rises as the temperature is lowered (approximately as $R = R_o e^{c/T}$; c, R_o constants) and its high dR/dT is related directly with its high resistance. In fact, for thin films the resistance of pure semiconductors in the liquid helium II temperature range is so high that doping them is necessary to make them usable. On the other hand,

the resistance of superconductors, which is generally low, drops to zero within a small temperature range at some transition temperature, T_c (defined as the temperature at which the resistance is half the normal resistance). Consequently, for impedance matching purposes and in order to minimize electromagnetic coupling between emitter and detector, thin film superconductors were used as the detectors for megacycle frequency second sound in this experiment.

A superconductor is useful as a second sound detector only over a small temperature range about its transition temperature, T_c, where its resistance changes from its normal value, R_n, to zero. Consequently, different superconductors with different transition temperatures were used to cover the entire liquid helium II temperature range above $1.2^{\circ}K$. In any one experiment second sound was investigated over only a small region of temperature. Although a very large number of superconductors can be used, the ones used for this experiment were films of the compound Au_2Bi[29-31] and superimposed Au-Sn[32] films.

Thin films of Au_2Bi were made by first evaporating approximately 600 Å of Bi on a 200 Å evaporated Au film, .075cm wide and 0.32cm long (both evaporations made at room temperatures). The resultant film was then placed in a pyrex vacuum cell and heated for one hour at about $250^{\circ}C$. This gave a thin film superconductor (Au_2Bi) with a normal resistance of 15Ω, a transition temperature of about $1.94^{\circ}K$, and a dR/dT (slope of resistance versus temperature curve) of about $700\Omega/^{\circ}K$ with 0.1 ma measuring current. (These values are approximate and are given only to indicate the

film's properties.) It was found during the investigation that variation of the amounts evaporated and the heating procedures permitted production of films which had transition temperatures anywhere from $1.2^{\circ}K$ to $2.2^{\circ}K$. The widths of the transitions occurring about $1.9^{\circ}K$ were very narrow, whereas transitions at appreciably lower or higher temperatures were not nearly so narrow. However, the primary value of a compound superconductor is to obtain easily a very high sensitivity near one temperature (in the case of Au_2Bi in the temperature range $1.8^{\circ}K$ - $2.1^{\circ}K$), a function performed very well by Au_2Bi.

The Au-Sn superimposed films were produced by evaporating (at room temperature) between 300 Å and 500 Å of Sn on 100 Å Au films. The transition temperature was a strong function of the ratio of Sn to Au thickness. For example, a 20 Å change in Sn thickness or a 10 Å change in Au thickness changed the transition temperature approximately $0.1^{\circ}K$. Furthermore, the length of evaporation and temperature of the boat effected the transition temperature. Consequently, in order to use superimposed films to obtain required transition temperatures reproducibly, it is necessary to be able to repeat, exactly, the evaporation conditions. On the average, it was found that for certain normal resistances it was possible to obtain certain dR/dT values

$R_N(\Omega)$	dR/dT $(\Omega/^{\circ}K)$
2.3	10
23	120
54	300 - 1200

where a measuring current of 0.1 ma was used. The normal resistances of the order of 54Ω were obtained for films 0.32 cm long and a length to width ratio of about 15. As seen from the values of dR/dT versus R_N, for very small films very narrow transitions can be obtained, approaching the value for transitions of compounds. However, the primary purpose of using these films is to obtain a good sensitivity over a fairly wide temperature range (approximately $0.2^{\circ}K$ in this case) and to be able to change the transition temperature easily. Both these functions are performed very well by Au-Sn superimposed films when proper care is taken in their fabrication.

The stability of some of the films was noted for approximately two-month periods with repeated cycling to liquid helium temperatures. The results showed that in general:

(1) The T_c and dR/dT of superimposed Au-Sn films decreased a little but not significantly.

(2) For Au_2Bi films with T_c inside the $1.8^{\circ}K$ - $2.0^{\circ}K$ range there was at most a slight change of T_c and dR/dT. However, films with higher T_c annealed to transition temperatures within the $1.8^{\circ}K$ - $2.0^{\circ}K$ range, while films with lower T_c also annealed to still lower transition temperatures till the superconducting properties were gone.

Consequently, by using Au-Sn superimposed films it is possible to make stable overlapping second sound detectors to cover the entire temperature range between $1.2^{\circ}K$ and $2.2^{\circ}K$ with good sensitivity, while for very high sensitivity at particular tempera-

tures, compounds (such as Au_2Bi at 1.8^oK to 2.0^oK) or very small Au-Sn films can be used.

Since Eq. (2) shows that the ratio between the voltage, ΔV, generated at the detector, and the second sound amplitude, ΔT_{ss}, is $I_o dR/dT$, this is the value which will be defined as the sensitivity of the detector. It is important that it be noted that dR/dT is a function of I_o (as is T_c) and decreases for very high values of I_o. Consequently, when determining $I_o dR/dT$ it is necessary that it be measured directly or that R versus T be measured under the exact conditions of the experiment. Values of the sensitivity are listed for the detectors with typical constant ac currents used in the experiment

Detector	$I_o dR/dT$ (amp $\Omega/^oK$)	I_o(ma)	$R_N(\Omega)$	$\Delta T_N(^oK)$
Au_2Bi	0.1 - 0.5	0.1 - 0.5	15	$6.5 - 1.3 \times 10^{-8}$
Au-Sn	0.01 - 0.05	0.1 - 0.5	23	$6.5 - 1.3 \times 10^{-7}$
Au-Sn (small)	0.03 - 0.1	0.1	54	$22 - 6.5 \times 10^{-8}$

Included with the sensitivity is a measure of the temperature fluctuation, ΔT_N, which gives a voltage at the detector equal to the noise of the electronic system at 1.28 Mc/sec which is 6.5×10^{-9} volts.

Finally it should be noted that the modulation of the rf voltage at the detector and the use of a four cycle wide wave analyzer provide a convenient means by which the electronic system

is narrowed to a four cycle bandwidth at all rf frequencies without requiring crystal controlled rf amplifiers and rf signal generators. It should be further realized that the most information (second sound signal) per power input by a detector current is obtained when only a constant ac current is used with no dc current. The rf signal then is not a truly modulated signal but rather just the two sidebands with no carrier. This is the condition found most desirable for second sound detection.

REFERENCES

[1] L. Tisza, J. Phys. Radium 1, 350 (1940).

[2] F. London, Superfluids (John Wiley and Sons, Inc., New York, 1954), Vol. 2.

[3] K. R. Atkins, Liquid Helium (Cambridge University Press, 1959).

[4] C. T. Lane, Superfluid Physics (McGraw-Hill Book Co., Inc., New York, 1962).

[5] G. Careri, Editor, Liquid Helium, Proceedings of the International School of Physics, Enrico Fermi (Academic Press, New York, 1963), Course 21.

[6] L. D. Landau, Zh. Eksperim. i Teor. Fiz. 11, 592 (1941).

[7] E. Lifshitz, Zh. Eksperim. i Teor. Fiz. 14, 116 (1944).

[8] V. P. Peshkov, Dokl. Akad. Nauk SSSR 45, 385 (1944).

[9] V. P. Peshkov, Zh. Eksperim. i Teor. Fiz. 16, 1000 (1946); 18, 438 (1948); 18, 857 (1948).

[10] A. J. Dessler and W. M. Fairbank, Phys. Rev. 104, 6 (1956).

[11] N. Kurti and J. McIntosh, Phil. Mag. 46, 104 (1955).

[12] R. D. Maurer and Melvin A. Herlin, Phys. Rev. 81, 444 (1951).

[13] C. T. Lane, Henry A. Fairbank, and William M. Fairbank, Phys. Rev. 71, 600 (1947).

[14] William M. Fairbank, Henry A. Fairbank, and C. T. Lane, Phys. Rev. 72, 645 (1947).

[15] J. R. Pellam, Phys. Rev. 75, 1183 (1949).

[16] D. V. Osborne, Nature 162, 213 (1948).

[17] J. Mercereau, H. Notarys, and J. R. Pellam, Proceedings of the VIIth International Conference on Low Temperature Physics, Edited by G. M. Graham and A. C. Hollis Hallett (University of Toronto Press, Canada, 1961) p. 552.

[18] K. R. Atkins and K. H. Hart, Can. J. Phys. 32, 381 (1954).

[19] W. B. Hanson and J. R. Pellam, Phys. Rev. 95, 321 (1954).

[20] K. N. Zinov'eva, Zh. Eksperim. i Teor. Fiz. 25, 235 (1953); 31, 31 (1956).

[21] L. D. Landau and I. M. Khalatnikov, Zh. Eksperim. i Teor. Fiz. 19, 637, 709 (1949).

[22] I. M. Khalatnikov, Zh. Eksperim. i Teor. Fiz. 20, 243 (1950); 23, 8 (1952).

[23] I. M. Khalatnikov, Zh. Eksperim. i Teor. Fiz. 23, 21 (1952).

[24] H. N. V. Temperley, Proc. Phys. Soc. (London) A64, 105 (1951).

[25] I. M. Khalatnikov, Dokl. Akad. Nauk SSSR 79, 237 (1951).

[26] I. M. Khalatnikov, Zh. Eksperim. i Teor. Fiz. 23, 253 (1952).

[27] Proceedings of the VIIth International Conference on Low Temperature Physics, edited by G. M. Graham and A. C. Hollis Hallett (University of Toronto Press, Canada, 1961) Chapter 20, p. 466.

[28] H. A. Snyder, Rev. Sci. Instr. 33, 467 (1962).

[29] M. Hansen, Constitution of Binary Alloys (McGraw-Hill Book Co., Inc., New York, 1958) p. 188.

[30] N. E. Alekseevskii, G. S. Zhdanov, and N. N. Zhuravlev, Zh. Eksperim. i Teor. Fiz. 25, 123 (1953).

[31] W. J. deHaas and T. Jurriaanse, Leiden Communications 220e (1932).

[32] W. A. Simmons and D. H. Douglass, Jr., Phys. Rev. Letters 9, 153 (1962).

[33] A. G. Fox and Tingye Li, BSTJ 40, 453 (1961).